

PRIDE: Path Integration Based Delay Estimation in Multi-Device Multi-Path Environments

Wei Peng , Senior Member, IEEE, Xuehui Zhao , Tao Jiang , Senior Member, IEEE, and Fumiyuki Adachi , Life Fellow, IEEE

Abstract—Massive connectivity in the near future puts forward an urgent demand for the accurate time delay estimation (TDE). However, the accuracy of the traditional TDE methods is severely degraded by the multi-path interference (MPI) and multi-device interference. In this paper, we propose a path integration based delay estimation (PRIDE) method. For the first time, the unique delay structure of each device is utilized, and the MPI is converted to an assistance. Considering the practical case where multi-path delays are non-integer times of the sampling period, PRIDE is carried out in two steps to estimate the integer and fractional parts of the delay sequentially. Theoretical analysis and simulations show that the TDE accuracy in the multi-device multi-path environment can be greatly improved by the proposed PRIDE method with comparatively low computational complexity.

Index Terms—Time delay estimation, path integration, multi-path, multi-device.

I. INTRODUCTION

IN RECENT years, the time delay estimation (TDE) has received great attention in various applications, including radio localization [1], radar detection [2], and wireless communication [3]. The delay information can be utilized for synchronization, which provides great help in systems with multiple devices. Especially, the number of devices connected to the wireless network is expected to reach five hundred billion by the year of 2020, and the efficient management of the massive connectivity puts an urgent demand for accurate TDE in complex environments. The wireless environment is generally characterized by the multi-path propagation. As a result, the signal energy is dispersive in both time and frequency domains, which makes it

difficult to distinguish the paths. For this reason, the multi-path environment is often considered unfriendly to the TDE.

Among traditional TDE methods, the cross-correlation (CC) based time domain estimation [4]–[8] is widely used. The CC method computes the cross-correlation between the received signal and the pilot signal, and the time delay is then determined through a first path search (FPS) by peak detection. However, the peak is easily affected by the noise, multi-path interference (MPI), as well as the multi-device interference (MDI). Especially, in the non-line-of-sight (NLOS) environment, the first path does not always correspond to the peak. As a result, CC based methods could hardly yield a good performance. An alternative of the CC method is proposed in [9], where a symmetric pilot signal is used so that the cross-correlation can be replaced by the auto-correlation of the received signal. However, the symmetric structure is broken in the time-selective channel and the auto-correlation based method turns out to be inefficient.

Generalized CC (GCC) based frequency domain estimation [10]–[14] is proposed to sharpen the CC peak by weighted multiplication in frequency domain. In this way, the effect of the noise can be suppressed. However, the performance is still far from satisfactory in the presence of MPI and MDI. In order to improve the estimation accuracy of TDE, the maximum likelihood (ML) based methods are proposed. By realizing the TDE through a full search to maximize the delay probability, ML based methods have been proposed in both time and frequency domains [15]–[18]. Theoretically, ML methods are more robust than the CC and GCC methods, however, their computational complexity is too high to be applied in real systems [19].

Practically speaking, the multi-path delays could be non-integer times of the sampling period, which makes the accurate TDE even more difficult. Without increasing the sampling rate, phase-shift searching based fractional delay estimation is proposed [20], [21]. However, satisfactory performance could only be obtained in the single-device single-path scenario. If we reconsider the multi-path environment, it is interesting to notice that, in most of the applications, the wireless devices are settled in a stable environment. E.g., the television, desktop, printer, and air conditioner that share the indoor WIFI links are almost fixed. In this case, we embrace a good side: the differences among the multi-path delays are only related to the limited scatters on each path, which remain unchanged within a relatively long time [22]. Defining the multiple delay differences of one device as its delay structure, the good news is that the delay structure of each device is unique.

Manuscript received April 18, 2018; revised July 13, 2018; accepted August 26, 2018. Date of publication September 24, 2018; date of current version December 14, 2018. This work was supported in part by National Science Foundation of China under Grants 61771214, 61771216, and 61531011, in part by the National Science Foundation for Distinguished Young Scholars of China under Grant 61325004, in part by the Innovative Project of Shenzhen City in China under Grant JCYJ20170307171931096, in part by the Open Research Fund of National Mobile Communications Research Laboratory, Southeast University under Grant 2018D10, and in part by the Fundamental Research Funds for the Central Universities under Grant 2015ZDTD012. The review of this paper was coordinated by Prof. Y. Li. (Corresponding author: Wei Peng.)

W. Peng, X. Zhao, and T. Jiang are with the School of Electronic Information and Communications, Huazhong University of Science and Technology, Wuhan 430074, China (e-mail: pengwei@hust.edu.cn; xuehuizhao@hust.edu.cn; Tao.Jiang@ieee.org).

F. Adachi is with the Tohoku University, Sendai 980-8576, Japan (e-mail: adachi@ecei.tohoku.ac.jp).

Color versions of one or more of the figures in this paper are available online at <http://ieeexplore.ieee.org>.

Digital Object Identifier 10.1109/TVT.2018.2872020

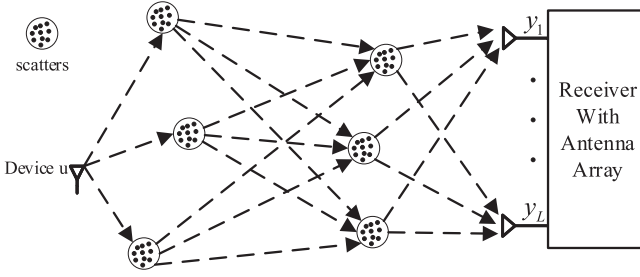


Fig. 1. System Model.

In this paper, for the first time, we utilize the delay structure in the TDE and propose a Path integRation based Delay Estimation (PRIDE) method. The multi-path delays of each device is represented by the first path delay and the delay structure. Then, the first path is reinforced by path integration so that it can be estimated with a high accuracy. The PRIDE method is carried out in two steps to obtain the integer and fractional parts of the delay in sequence. In addition, the multi-path delays obtained by the PRIDE method is used for the angle of arrival (AOA) estimation, and theoretical analysis on the root-mean-square-error (RMSE) is carried out. Simulation results verify the effectiveness of the proposed method. It is shown that, a significant improvement in the TDE accuracy can be obtained by the PRIDE method when compared with the existing methods. In addition, the spatial diversity is employed and a performance improvement is observed as the number of antennas increases.

The rest of this paper is organized as follows. Section II presents the system model. Starting from the single-device single-path scenario, the traditional TDE methods are briefly introduced in Section III. Then, the PRIDE method is proposed for the multi-device multi-path scenario in Section IV. The PRIDE based AOA estimation is proposed and its RMSE is analyzed in Section V. Simulation results are presented in Section VI and conclusions are given in Section VII.

II. THE SYSTEM MODEL

In this paper, an uplink multi-device communication system with multiple antennas is considered. The base station is equipped with an L -antenna array, and there are U single-antenna devices. Taking the u th device as an example, the system model is shown in Fig. 1.

The discrete equivalent baseband received signal at any antenna (the antenna index is omitted for simplicity) is given as

$$y[n] = \sum_{u=1}^U h_u[n] * x_u[n] + w[n], \quad (1)$$

where $y[n]$ and $x_u[n]$ respectively denote the received and transmitted sequence, $w[n]$ is the additive white Gaussian noise with zero-mean and variance σ^2 , $*$ denotes the convolution operation, and $h_u[n]$ represents the multi-path channel fading, given as

$$h_u[n] = \sum_{i=1}^{P_u} \alpha_{u,i} \delta[n - \tau_{u,i}], \quad (2)$$

where P_u is the number of multiple paths, δ stands for the delta function, $\alpha_{u,i}$ and $\tau_{u,i}$ represent the fading coefficient and the delay time of the i th path, respectively. In this paper, we consider a stable environment, and the delay differences between multiple paths change slowly. Thus, the multi-path delays of device u can be represented as

$$\boldsymbol{\tau}_u = [\tau_{u,1} + t_{u,1}, \dots, \tau_{u,1} + t_{u,i}, \dots, \tau_{u,1} + t_{u,P_u}], \quad (3)$$

where $\boldsymbol{\tau}_u$ represents the vector of multi-path delays, $\tau_{u,1}$ denotes the delay time of the first path, and $t_{u,i} = \tau_{u,i} - \tau_{u,1}$ represents the time difference between the i th path and the first path. We define the delay structure of device u as \boldsymbol{S}_u , given as

$$\boldsymbol{S}_u = [t_{u,1}, \dots, t_{u,i}, \dots, t_{u,P_u}]. \quad (4)$$

Then, $\boldsymbol{\tau}_u$ can be rewritten as

$$\boldsymbol{\tau}_u = \tau_{u,1} \mathbf{1} + \boldsymbol{S}_u, \quad (5)$$

where $\mathbf{1}$ represents the all-one vector of length P_u . It is indicated by (5) that once the delay time of the first path is obtained, we can get the delay time of the other paths directly. Note that, in the limited scattering environment, the delay structure is unique for each device. Hereafter, the delay structure is used as the priori knowledge, which might be obtained through orthogonal pilot sequence with sufficiently large power in the training phase.

III. DELAY ESTIMATION IN THE SINGLE-DEVICE SINGLE-PATH ENVIRONMENT

In this section, we give a brief introduction to traditional TDE methods in the single-device single-path environment, where (1) is simplified as

$$y[n] = h[n] * x[n] + w[n], \quad (6)$$

where $h[n] = \alpha \delta[n - \tau]$, α and τ represent the fading coefficient and the delay time, respectively.

A. Time Domain TDE

The received signal is a delayed and distorted replica of the transmitted signal in the time domain. Therefore, the cross-correlation of them can be used to obtain the delay estimation, given as

$$R_{cc}[m] = \sum_{n=0}^{N-1} x^\dagger[n] y[n+m], \quad (7)$$

where N represents the sequence length and \dagger denotes the conjugate operation. Substituting (6) into (7), we have

$$R_{cc}[m] = \alpha R_{xx}[m - \tau] + R_{xw}[m], \quad (8)$$

where R_{xx} represents the auto-correlation of $x[n]$, and R_{xw} denotes the cross-correlation between $x[n]$ and $w[n]$. It is clear that $\lim_{N \rightarrow \infty} R_{xw}[m] = 0$. Thus, given a large value of N , (8) can be re-written as

$$R_{cc}[m] = \alpha R_{xx}[m] * \delta[m - \tau]. \quad (9)$$

It is implied by (9) that $R_{cc}[m]$ is a delayed replica of $R_{xx}[m]$. Therefore, the TDE can be obtained as

$$\hat{\tau}_{cc} = \arg \max_m R_{cc}[m]. \quad (10)$$

B. Frequency Domain TDE

The phase-only correlation (POC) based method is taken as an example, by which the frequency domain product of the transmitted and received signals is normalized and only the phase information is remained, given as

$$r[k] = \frac{\alpha |X[k]|^2 e^{-j\frac{2\pi}{N}k\tau} + X^\dagger[k]W[k]}{|X[k]| |\alpha X[k] e^{-j\frac{2\pi}{N}k\tau} + W[k]|}, \quad (11)$$

where $X[k]$, $Y[k]$, and $W[k]$ respectively denote the frequency-domain counter-parts of $x[n]$, $y[n]$, and $w[n]$. $|\cdot|$ represents the modulus operation. For convenience, the noise term in (11) is omitted and the equation is simplified as

$$\underline{r[k]} = e^{-j\frac{2\pi}{N}k\tau}. \quad (12)$$

It is clear that the time domain representation of (12) is

$$R_{poc}[m] = \delta[m - \tau], \quad (13)$$

where $R_{poc}[m]$ is the inverse fast Fourier transform (IFFT) of $r[k]$. Then, the TDE is obtained as

$$\hat{\tau}_{poc} = \arg \max_m R_{poc}[m]. \quad (14)$$

IV. PROPOSED PRIDE METHOD IN THE MULTI-DEVICE MULTI-PATH ENVIRONMENT

Considering the general case where the delay time is non-integer times of the sampling interval, the delay time for the i^{th} path of device u can be represented as

$$\tau_{u,i} = \tau_{u,i}^I + \tau_{u,i}^F, \quad (15)$$

where $\tau_{u,i}^I$ is the integer part, equalling to the rounded-off $\tau_{u,i}$, given as

$$\tau_{u,i}^I = \text{round}(\tau_{u,i}), \quad (16)$$

and $\tau_{u,i}^F \in [-0.5, 0.5]$ is the fractional part, equaling to the difference between $\tau_{u,i}$ and $\tau_{u,i}^I$.

Based on (15), we propose a PRIDE method consisting of two steps.

Step 1: Estimation of the integer part $\tau_{u,i}^I$.

Step 2: Estimation of the fractional part $\tau_{u,i}^F$.

In the next, the two steps will be presented in sequence.

A. Integer Delay Estimation

Instead of treating the multiple paths separately, the proposed method integrate the multi-path components. Generally, PRIDE can be applied in conjunction with the traditional methods. Taking the CC method as an example, the principle of PRIDE-CC is shown in Fig. 2. Considering the u^{th} device, the cross-correlation \mathbf{R}_u obtained by the CC method is shown in Fig. 2(a). We apply the PRIDE method and obtain the integrated cross-correlation,

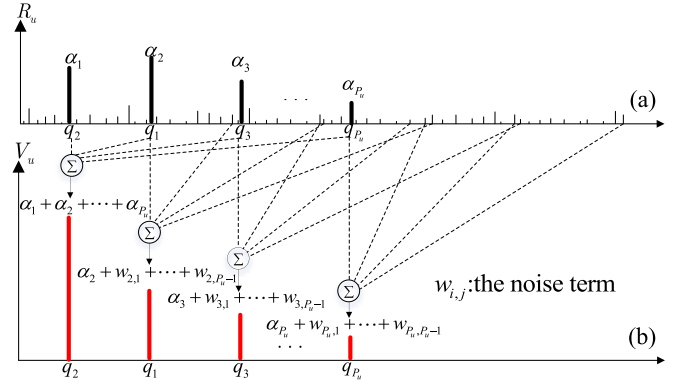


Fig. 2. Principle of PRIDE-CC.

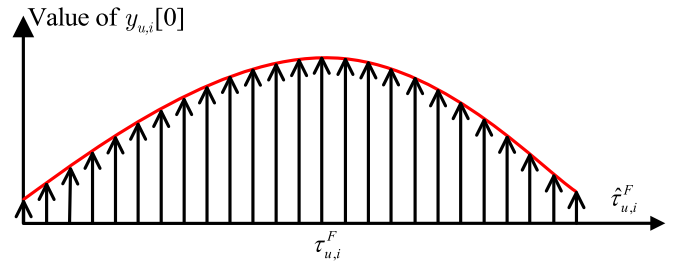


Fig. 3. Principle of fractional delay estimation.

as shown in Fig. 2(b). It is clear that the first path is reinforced and can then be easily detected. The details are presented as follows.

Firstly, we determine the candidates for the delay time of the first path by sorting \mathbf{R}_u in a descending order. The sorted sequence is denoted as

$$\tilde{\mathbf{R}}_u = [R_{cc}[q_{u,1}], R_{cc}[q_{u,2}], \dots, R_{cc}[q_{u,i}], \dots], \quad (17)$$

where $q_{u,i}$ is the index of the i^{th} largest value in \mathbf{R}_u . The vector of indexes corresponding to the top P_u values in $\tilde{\mathbf{R}}_u$ is denoted as

$$\mathbf{q}_u = [q_{u,1}, q_{u,2}, \dots, q_{u,P_u}]. \quad (18)$$

Substituting (18) into (5), the i^{th} candidate for τ_u could be obtained as

$$\mathbf{C}_{u,i} = q_{u,i} \mathbf{1} + \mathbf{S}_u. \quad (19)$$

The vector-form cross-correlation corresponding to the i^{th} multi-path delay candidate is denoted as

$$\mathbf{v}_{u,i} = [v_{u,i,1}, v_{u,i,2}, \dots, v_{u,i,P_u}], \quad (20)$$

where $v_{u,i,j} = R_{cc}[q_{u,i} + t_{u,j}]$ and $j = 1, 2, \dots, P_u$. Then, the vector of integrated cross-correlation of device u can be obtained by the summation over (20), given as

$$\mathbf{V}_u = [\text{sum}(\mathbf{v}_{u,1}), \text{sum}(\mathbf{v}_{u,2}), \dots, \text{sum}(\mathbf{v}_{u,P_u})], \quad (21)$$

where

$$\text{sum}(\mathbf{v}_{u,i}) = \sum_{j=1}^{P_u} v_{u,i,j}. \quad (22)$$

Next, the index of the first path is obtained by locating the peak value of \mathbf{V}_u , given as

$$I_u = \text{findmax}(\mathbf{V}_u). \quad (23)$$

Substituting I_u into (18), the integer delay of the first path is given as

$$\hat{\tau}_{u,1}^I = q_{u,I_u}. \quad (24)$$

Then, the integer multi-path delays of device u are obtained by substituting (24) into (5), given as

$$\hat{\tau}_u^I = \hat{\tau}_{u,1}^I \mathbf{1} + \mathbf{S}_u. \quad (25)$$

Discussion: In the example shown by Fig. 2, the first path does not yield the largest cross-correlation due to the propagation environment. In this case, the traditional methods will produce a wrong decision. After the path integration, the first path is empowered an augmented value. Obviously, if $q_{u,i} \neq \tau_{u,1}$, then $q_{u,i} + t_{u,i} \neq \tau_{u,i}$, and it is quite possible that $\mathbf{R}_u[q_{u,i} + t_{u,i}]$ corresponds to the noise term with a small value. Thus, for candidates from the other paths, the integrated cross-correlation in (22) turns out to be almost the same as the traditional one. Therefore, the first path can be easily distinguished and the probability of wrong estimation by (24) is greatly reduced.

B. Fractional Delay Estimation

According to (1) and (2), the frequency domain received signal of device u can be expressed as

$$Y_u[k] = \sum_{i=1}^{P_u} \alpha_{u,i} X_u[k] e^{-j \frac{2\pi}{N} k \tau_{u,i}} + W[k], \quad (26)$$

where $X_u[k] = \sum_{n=1}^N x_u[n] e^{-j \frac{2\pi}{N} k n}$ and $W[k] = \sum_{n=1}^N w[n] e^{-j \frac{2\pi}{N} k n}$. In the following, the noise term is omitted for simplicity.

Lemma 1: Defining a sequence of shifted response $Y'_{u,i}$, given as

$$Y'_{u,i}[k] = \frac{Y_u[k]}{X_u[k]} e^{j \frac{2\pi}{N} k \hat{\tau}_{u,i}}. \quad (27)$$

The estimated fractional delay, denoted as $\hat{\tau}_{u,i}^F$, will yield a peak of $y_{u,i}[n]$ at $n = 0$ when $\hat{\tau}_{u,i}^F = \tau_{u,i}^F$, where

$$y_{u,i}[n] = \frac{1}{N} \sum_{k=1}^N Y'_{u,i}[k] e^{j \frac{2\pi}{N} k n}. \quad (28)$$

Proof: Substituting X_u and Y_u into (27), we have

$$Y'_{u,i}[k] = \alpha_{u,i} e^{-j \frac{2\pi}{N} k (\tau_{u,i} - \hat{\tau}_{u,i})} + \sum_{j \neq i} \alpha_{u,j} e^{-j \frac{2\pi}{N} k (\tau_{u,j} - \hat{\tau}_{u,i})}. \quad (29)$$

Assuming that the integer delay estimation is accurate, it is direct that if the fractional delay estimation is also accurate, then $\hat{\tau}_{u,i} = \tau_{u,i}$ and (29) becomes

$$Y'_{u,i}[k] = \alpha_{u,i} + \sum_{j \neq i} \alpha_{u,j} e^{-j \frac{2\pi}{N} k (\tau_{u,j} - \hat{\tau}_{u,i})}. \quad (30)$$

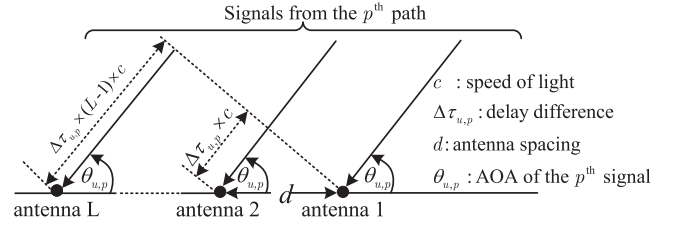


Fig. 4. Received signals at the antenna array.

Then, the sequence $y_{u,i}[n]$ is obtained by substituting (30) into (28), given as

$$y_{u,i}[n] = \alpha_{u,i} \delta[n] + z_i[n], \quad (31)$$

where

$$z_i[n] = \frac{1}{N} \sum_{k=1}^N \sum_{j \neq i} \alpha_{u,j} e^{-j \frac{2\pi}{N} k (\tau_{u,j} - \hat{\tau}_{u,i})} e^{j \frac{2\pi}{N} k n}. \quad (32)$$

Now, it is clear that the peak of $y_{u,i}[0]$ appears when $\hat{\tau}_{u,i}^F = \tau_{u,i}^F$, as shown in Fig. 4.

Therefore, the fractional delay estimation is equivalent to finding the value of $\hat{\tau}_{u,i}^F$ that maximizes $y_{u,i}[0]$, given as

$$\hat{\tau}_{u,i}^F = \arg \max_{\tau_{u,i}^F} y_{u,i}[0]. \quad (33)$$

Similar to the integer path delay estimation, we also apply the PRIDE principle in the searching process for $\hat{\tau}_{u,i}^F$. Denoting the number of fractions as N_F , the candidates for the fractional delay $\tau_{u,i}^F$ of the first path is given as

$$f_{u,1,n_F} = -0.5 + \frac{n_F}{N_F}, \quad (34)$$

where $n_F = 0, 1, \dots, N_F$. Then, we can get the candidates for the delay time of the first path by substituting (34) and (24) into (15), given as

$$\hat{\tau}_{u,1,n_F} = \hat{\tau}_{u,1}^I + f_{u,1,n_F}. \quad (35)$$

Applying the path integration, the sequence of the integrated time domain delayed response is calculated as

$$y'_{u,n_F}[n] = \sum_{i=1}^{P_u} y_{u,i,n_F}[n], \quad (36)$$

where

$$y_{u,i,n_F}[n] = \alpha_{u,i} \delta[n] + z_i[n]. \quad (37)$$

Then, the delay estimation for the first path is obtained as

$$\hat{\tau}_{u,1} = \arg \max_{\hat{\tau}_{u,1,n_F}} y_{u,i,n_F}[0]. \quad (38)$$

The estimated multi-path delays of device u in the vector form are obtained by substituting (38) into (5), given as

$$\hat{\tau}_u = \hat{\tau}_{u,1} \mathbf{1} + \mathbf{S}_u. \quad (39)$$

Note that, taking the above illustration for device u as an example, the proposed PRIDE method can be applied for the TDE of each device. Therefore, the multi-device multi-path TDE

TABLE I
 VARIABLES OF THE PRIDE METHOD FOR THE DEVICE u

Variables	Descriptions
S_u	Time delay structure
R_u	The cross-correlation sequence
\tilde{R}_u	Sequence of the re-sorted cross-correlation in descending order
$q_{u,i}$	The index of the i^{th} largest value in R_u
q_u	Vector of candidates for the first path integer delay
$C_{u,i}$	The i^{th} candidate of the multi-path delay vector
$v_{u,i,j}$	The $(q_{u,i} + t_{u,j})^{\text{th}}$ element of R_u
$v_{u,i}$	Vector form cross-correlation corresponding to $C_{u,i}$
V_u	Vector of integrated cross-correlation
I_u	Index of the peak in V_u
$\hat{\tau}_{u,1}^I$	Estimated first path integer delay
$\hat{\tau}_u^I$	Vector of estimated integer multi-path delay
$Y_u[k]$	Frequency domain received signal
$X_u[k]$	Frequency domain transmitted signal
$Y'_{u,i}[k]$	Frequency domain shifted response
$y_{u,i}[n]$	Time domain delayed response of the i^{th} path
$\hat{\tau}_{u,i}^F$	Estimated fractional delay
N_F	Number of fractions for fractional delay estimation
$f_{u,1,n_F}$	The n_F^{th} candidate of the first path fractional delay
$\hat{\tau}_{u,1,n_F}$	The n_F^{th} candidate of the first path delay
$y_{u,i,n_f}[n]$	Time domain delayed response of the i^{th} path for the n_f^{th} delay candidate
$y'_{u,n_f}[n]$	Integrated time domain delayed response
$\hat{\tau}_{u,1}$	The estimated first path delay
$\hat{\tau}_u$	The estimated multi-path delay vector

can be realized. In summary, the variables and necessary steps of the PRIDE algorithm are listed in Table I and Algorithm 1, respectively.

V. APPLICATION OF THE PRIDE METHOD TO AOA ESTIMATION

A. PRIDE Based AOA Estimation

An important application of the time delay estimation is to obtain the AOA. In this part, we present the PRIDE based AOA estimation in the multi-device multi-path environment, where a unitary linear antenna array (ULA) is used.

Algorithm 1: Path integration Based Delay Estimation.

Input:

The pilot sequence $x_u[n]$ and received sequences $y[n]$;
 The delay structure S_u ;

Output:

The estimated multi-path delay vector $\hat{\tau}_u$;

1: First path integer delay estimation:

- 2: Determine the candidates of $\tau_{u,1}^I$ following (19);
- 3: Calculate the integrated cross-correlation following (21).
- 4: Find the peak of the integrated cross-correlation and obtain the integer delay estimation following (24);

5: First path fractional delay estimation:

- 6: Determine the candidates of $\tau_{u,1}^F$ following (34);
- 7: Calculate the integrated time domain response for $n = 0$ following (36);
- 8: Find the peak of the integrated time domain response and complete the delay estimation following (38);

9: Multi-path delay estimation:

- 10: Obtain the multi-path delay vector following (39).

Under the far field transmission assumption, the wavefront of any signal path will arrive at the antenna array in a planer form. Therefore, the time of arrivals (TOAs) belonging to neighboring antennas imply a delay difference determined by both the antenna spacing and the AOA, as show in Fig 4.

Denoting the AOA associated with the p th path of device u as $\theta_{u,p}$, and the delay difference between two adjacent antennas as $\Delta\tau_{u,p}$, we have

$$\Delta\tau_{u,p} = \frac{d}{c} \cos \theta_{u,p}, p = 1, 2, \dots, P_u, \quad (40)$$

where c is the speed of light, and d is the distance between the neighboring antennas.

Given (40), the delay time of the p th path on the l th antenna can be given as

$$\tau_{u,p,l} = \tau_{u,p,1} + (l-1)\Delta\tau_{u,p}, \quad (41)$$

where $\tau_{u,p,1}$ is the delay time of the p th path on antenna 1.

By applying the PRIDE method, we can obtain the delay time of the p th path on each antenna, denoted as $\hat{\tau}_{u,p,1}, \dots, \hat{\tau}_{u,p,L}$ respectively. In order to obtain the delay difference between neighboring antennas, the least square linear fitting is applied on the estimated time delays, where a cost function is used, given as

$$J(\tau_{u,p,1}, \Delta\tau_{u,p}) = \sum_{l=1}^L (\hat{\tau}_{u,p,l} - \tau_{u,p,1} - (l-1)\Delta\tau_{u,p})^2. \quad (42)$$

To minimize (42), we have

$$\begin{cases} \frac{\partial J}{\partial \tau_{u,p,1}} = 0, \\ \frac{\partial J}{\partial \Delta\tau_{u,p}} = 0, \end{cases} \quad (43)$$

where ∂ stands for the partial derivative. Substituting (42) into (43), we have

$$\begin{cases} -\sum_{l=1}^L 2[\hat{\tau}_{u,p,l} - \tau_{u,p,1} - (l-1)\Delta\tau_{u,p}] = 0 \\ -\sum_{l=1}^L 2(l-1)[\hat{\tau}_{u,p,l} - \tau_{u,p,1} - (l-1)\Delta\tau_{u,p}] = 0 \end{cases} \quad (44)$$

By solving (44), the estimation of $\tau_{u,p,1}$ and $\Delta\tau_{u,p}$, which are respectively represented as $\hat{\tau}_{u,p,1}$ and $\hat{\Delta}\tau_{u,p}$, can be obtained, given as

$$\hat{\tau}_{u,p,1} = \frac{2}{L(L+1)} \sum_{l=1}^L [(2L-1) - 3(l-1)] \hat{\tau}_{u,p,l}, \quad (45)$$

and

$$\hat{\Delta}\tau_{u,p} = \frac{12}{L(L^2-1)} \sum_{l=1}^L \left[(l-1) - \frac{L-1}{2} \right] \hat{\tau}_{u,p,l}. \quad (46)$$

According to (40), we have

$$\theta_{u,p} = \arccos \left(\Delta\tau_{u,p} \frac{c}{d} \right). \quad (47)$$

Substituting (46) into (47), the estimation of $\theta_{u,p}$ can be obtained, given as

$$\hat{\theta}_{u,p} = \arccos \left(\hat{\Delta}\tau_{u,p} \frac{c}{d} \right). \quad (48)$$

B. RMSE Analysis

The RMSE of $\hat{\Delta}\tau_{u,p}$ can be calculated as

$$\text{RMSE}_{\Delta\tau_{u,p}} = \sqrt{\frac{1}{N_{\text{total}}} \sum_{i=1}^{N_{\text{total}}} \left(\hat{\Delta}\tau_{u,p}^i - \Delta\tau_{u,p} \right)^2}, \quad (49)$$

where N_{total} is the sampling size. Denoting the estimated delay $\hat{\tau}_{u,p,l}$ as

$$\hat{\tau}_{u,p,l} = \tau_{u,p,l} + \gamma_{u,p,l}, \quad (50)$$

where $\gamma_{u,p,l}$ is a random variable with variance σ_γ^2 . Substituting (46) and (50) into (49), $\text{RMSE}_{\Delta\tau_{u,p}}$ is given as

$$\text{RMSE}_{\Delta\tau_{u,p}} = \sqrt{\frac{12}{L(L^2-1)}} \sigma_\gamma. \quad (51)$$

Then, substituting (51) into (48), the RMSE of $\hat{\theta}_{u,p}$ is obtained as [23]

$$\text{RMSE}_{\theta_{u,p}} = \frac{f(\theta_{u,p}, \sigma_\gamma)}{d\sqrt{L(L^2-1)}}, \quad (52)$$

where $f(\theta_{u,p}, \sigma_\gamma) = 2\sqrt{3}c\sigma_\gamma/\sin\theta_{u,p}$. It is indicated by (52) that, given σ_γ and $\theta_{u,p}$, the RMSE of the PRIDE based AOA estimation can be reduced by increasing d and L . Specifically, the array size of the ULA is $D_{\text{array}} = (L-1)d$. As L increases, we have

$$\lim_{L \rightarrow \infty} d\sqrt{L(L^2-1)} = \sqrt{L}D_{\text{array}}. \quad (53)$$

Substituting (53) into (52), we have $\lim_{L \rightarrow \infty} \text{RMSE}_{\theta_{u,p}} = f(\theta_{u,p}, \sigma_\gamma)/\sqrt{L}D_{\text{array}}$.

TABLE II
SIMULATION PARAMETERS

Path	1	2	3	4	5
Gain	0	-8	-10	-12	-18
Delay	2	5.2	2.8	19.2	51.2

VI. SIMULATION RESULTS

In this section, the performance of the proposed PRIDE method is testified by Monte-Carlo simulations and some representative results are presented. At first, the accuracy rate of the proposed PRIDE for integer delay estimation is testified, which is evaluated by $\rho = N_{\text{correct}}/N_{\text{total}}$, where N_{correct} is the number of accurate estimations and $N_{\text{total}} = 10000$ is the number of Monte-Carlo runs. Then, the performance of fractional delay estimation is testified when PRIDE is applied for AOA estimation with fractional delay time difference between neighboring antennas. The RMSE of the AOA estimation is evaluated with respect to the signal-to-noise-ratio (SNR), number of antennas, antenna spacing and AOA, respectively.

The parameters for simulations are as follows. For the integer delay estimation, the multi-path delays in ns and corresponding path gains in dB are listed in Table II, where T_s represents the sampling interval. The sampling frequency adopted in this paper is $F_s = 2.5$ GHz and value of the sampling interval can be calculated $T_s = 0.4$ ns. For the PRIDE based AOA estimation, the AOA of each path is randomly generated as a Laplacian variable, the mean value of which uniformly distributes within $(0, \pi)$, and the standard deviation is $\pi/36$.

A. Time Delay Estimation

In this subsection, the proposed PRIDE method is applied in conjunction with the CC and POC methods for integer delay estimation, respectively denoted as PRIDE-CC and PRIDE-POC. The performance of the traditional TDE methods, including grid search ML, FPS based CC and POC (respectively denoted as GS-ML [15], FPS-CC [10] and FPS-POC [12]), are also presented for comparison. The single-device case is considered at first and the multi-device case is studied in the next.

- *Single device case:* The estimation accuracy rate of the PRIDE method in the single-device case is shown in Fig. 5. It is observed that: 1) Among the traditional methods, GS-ML can obtain the best performance in the high-SNR region, while FPS-CC achieves the best performance in the low-SNR region. Specifically, the accuracy rate of GS-ML is outperformed by FPS-CC when $\text{SNR} < -11$ dB, where it is severely degraded by the noise. 2) The TDE performance can be significantly improved by the proposed method when compared with the best one of the traditional methods. For example, the accuracy rate is increased from 0.63 to 0.90 when $\text{SNR} = -12$ dB, and an improvement from 0.91 to 0.99 is achieved when $\text{SNR} = -8$ dB. In addition, the SNR requirement for an error-free TDE is -6 dB for the proposed method, while it is 0 dB for GS-ML. It should be noted that, as a practical consideration,

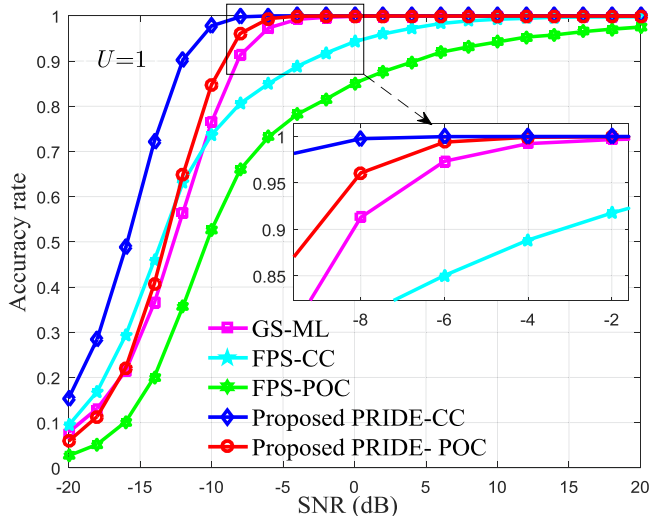


Fig. 5. Accuracy rate of the integer delay estimation, single-device case.

the computational complexity of the PRIDE method is slightly higher than FPS-CC or FPS-POC, while it is much lower than GS-ML. This will be analyzed later in Subsection VI-C.

Discussion: Due to the noise and interference, the peak of the first path may not be the largest one among all the paths, and traditional methods may wrongly choose the largest peak as the first path. Different from the traditional way, the proposed method choose several candidates for the first path. By employing the delay structure and integrating the path energy, the first path will be augmented while the other paths will remain almost unchanged. Then the first path will be easily recognized and the error probability is greatly reduced. Therefore, the TDE performance can be improved more by the proposed method as compared to the traditional methods.

A root mean square error (RMSE) comparison between the proposed method and the subspace-based methods such as multiple signal classification (MUSIC) [27] and signal parameters via rotational invariance technique (ESPRIT) [28] is shown in Fig. 6, and the Cramer-Rao bound (CRB) is also given as a reference. It is observed that, the proposed PRIDE method has a much lower RMSE than MUSIC or ESPRIT, and its RMSE gets very close to the CRB as the SNR increases.

- *Multi-Device Case:* The MDI will degrade the performance of TDE and the estimation accuracy rate of the PRIDE method in the multi-user case is shown in Fig. 7, where $\text{SNR} = 5$ dB and a maximum of ten users are used. The delay and path gain parameters are shown in Table III. It is observed that the traditional methods all experience a rapid accuracy decrease when the number of devices increases. Specifically, even the GS-ML method has a poor accuracy rate $\rho = 0.73$ when $U = 2$. Namely, taking $\rho \geq 0.9$ as the criterion, all the traditional methods fail to yield accurate TDE in the multi-device scenario. This is due to the fact that the MDI increases proportionally as the number of devices. However, the advantage

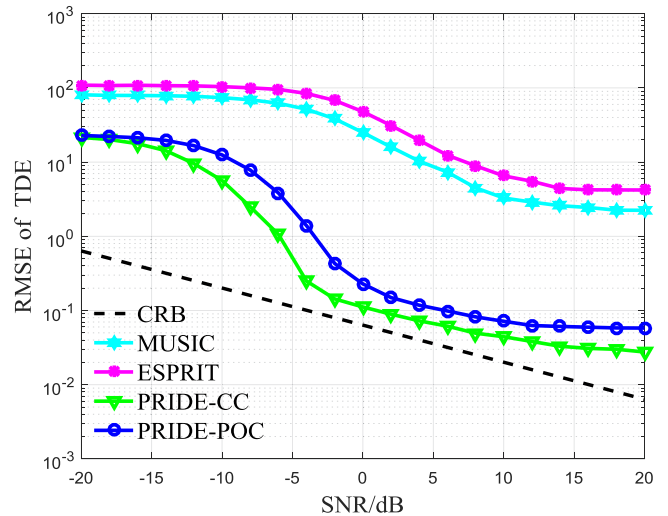


Fig. 6. RMSE of the PRIDE based TDE.

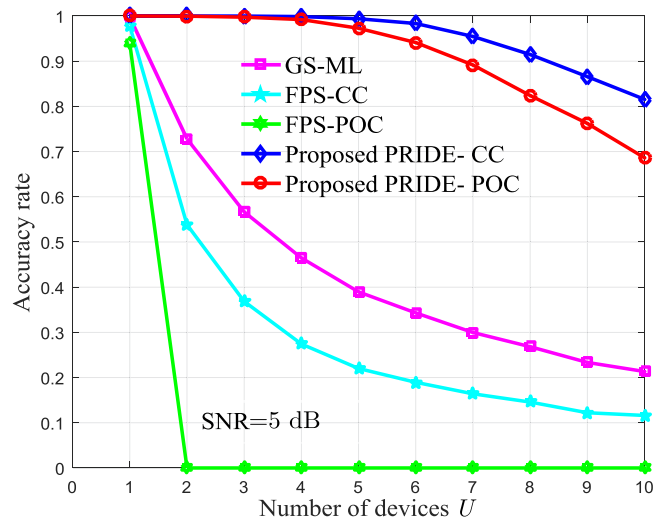


Fig. 7. Accuracy rate of the integer delay estimation, multi-device case.

of the PRIDE method is still significant. It is seen from Fig. 7 that, the accuracy of PRIDE-CC and PRIDE-POC decreases slowly as the number of devices increases. In addition, the PRIDE-CC method can yield accurate TDE for at most 8 devices.

B. AOA Estimation

According to (52), the RMSE of the PRIDE based AOA estimation is determined by the TDE error, the number of antennas L , antenna spacing d , and AOA $\theta_{p,u}$. In this subsection, we testify the effect of these parameters on the RMSE performance, respectively.

- *Effect of SNR*

The effect of SNR on the RMSE is shown in Fig. 8, where the number of antennas is $L = 2$ and the antenna spacing is 0.25 m. It can be observed that: 1) As the SNR increases, the TDE error reduces and the RMSE decreases. This is naturally straightforward and is also indicated by (52). 2)

TABLE III
MULTI-PATH PARAMETERS OF MULTIPLE DEVICES

Device	Path	1	2	3	4	5
1	Gain	-1.9	-7.3	-9.5	-14.4	-16.0
	Delay	2	5.2	10.8	19.2	51.2
2	Gain	-2.0	-7.5	-9.7	-12.9	-15.3
	Delay	2	8.8	11.6	38.4	60.4
3	Gain	-2.6	-6.7	-9.1	-10.0	-21.1
	Delay	2.4	18.4	18.8	56.4	77.6
4	Gain	-3.6	-3.7	-10.4	-14.7	-18.8
	Delay	3.2	4.4	18.4	36.4	46.8
5	Gain	-4.8	-5.2	-7.0	-8.6	-15.5
	Delay	1.2	15.6	29.6	45.6	60
6	Gain	-3.5	-6.1	-7.8	-8.8	-19.6
	Delay	4.4	38.8	45.6	60.8	78
7	Gain	-4.1	-5.1	-8.2	-9.1	-15.5
	Delay	2.8	25.2	50.8	51.2	62
8	Gain	-2.3	-6.1	-11.0	-12.9	-14.4
	Delay	5.6	21.6	30.8	59.6	62.8
9	Gain	-4.5	-5.2	-7.6	-9.1	-13.6
	Delay	5.2	64.4	73.2	75.2	76.4
10	Gain	-2.1	-8.7	-9.4	-9.7	-15.7
	Delay	6.4	43.2	43.6	47.2	53.6

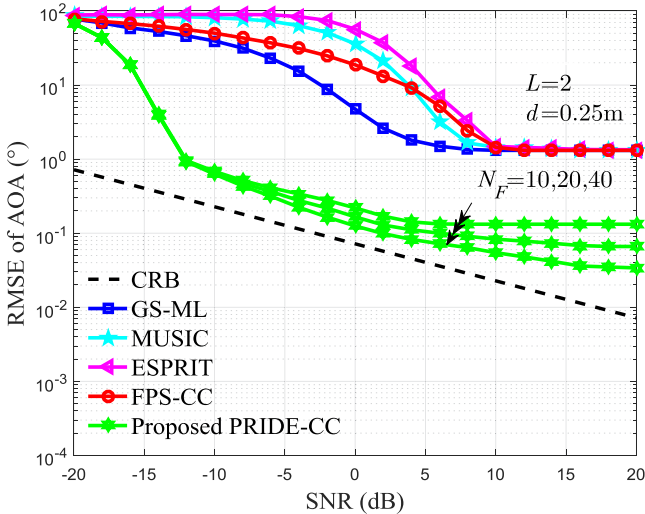


Fig. 8. RMSE of the PRIDE based AOA estimation vs SNR.

As the SNR increases, error floors appear with both the traditional and proposed methods. However, the reasons for them are different. Remember that the AOA estimation is affected by the TDE error. For the traditional TDE methods, the TDE accuracy is limited by the noise level as well as the sampling rate. For the proposed method, the TDE error is mainly determined by the searching precision. I.e., the RMSE floor of the traditional methods is fixed, while it is controllable by the proposed method. 3) The RMSE of AOA estimation is reduced by an order of magnitude when $N_F = 10$, and can be further improved by increasing the value of N_F , as shown in Fig. 8.

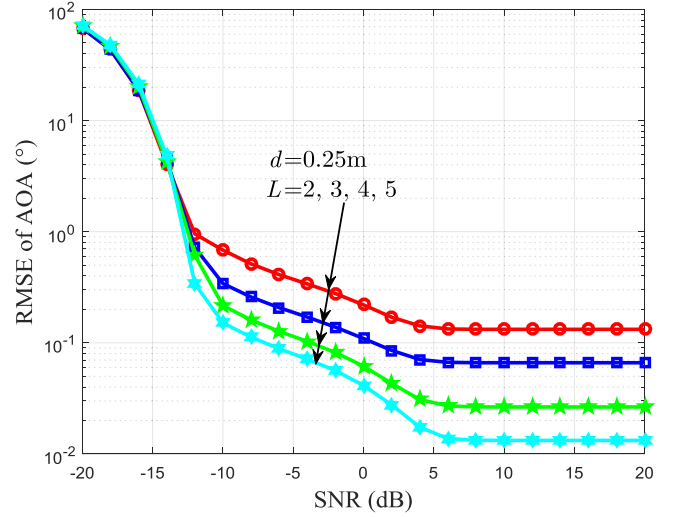


Fig. 9. RMSE of the PRIDE based AOA estimation vs the antenna number, $d = 0.25$ m.

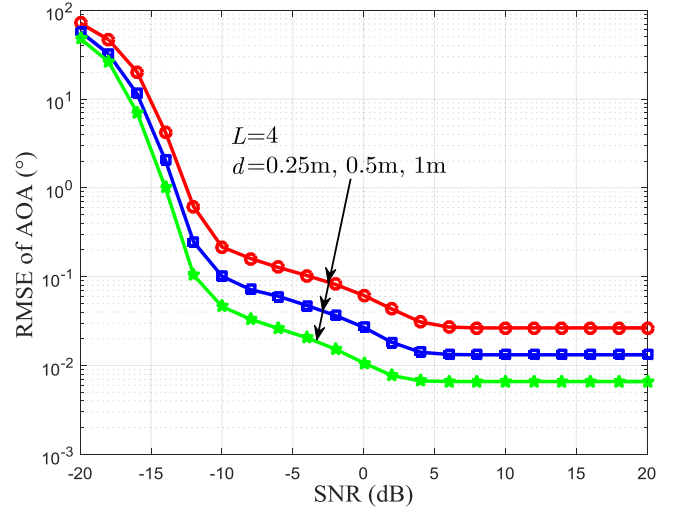


Fig. 10. RMSE of the PRIDE based AOA estimation vs the antenna spacing, $L = 4$.

- Effects of Antenna Number and Spacing

The effect of the antenna number on the RMSE is shown in Fig. 9, where $L \in \{2, 3, 4, 5\}$ and the antenna spacing is fixed as $d = 0.25$ m. Then, the effect of the antenna spacing is shown in Fig. 10, where $d \in \{0.25 \text{ m}, 0.5 \text{ m}, 1 \text{ m}\}$ [23] and the antenna number is fixed as $L = 4$. As indicated by (52), the RMSE of AOA estimation can be improved by increasing the antenna number as well as the antenna spacing, this is also verified by the results in Figs. 9 and 10. Taking the result at SNR = 0 dB as an example, the RMSE with $\{L = 2, d = 0.25 \text{ m}\}$ is 0.22, by increasing L to four, the RMSE is reduced to 0.06, and it is further reduced to 0.01 when we keep increasing d to 1 m.

- Effect of AOA

The effect of the AOA value on the RMSE is shown in Fig. 11, where $L = 4$, $d = 0.25$ m, and $N_F = 10$. Especially, SNR = 20 dB is used in order to eliminate the

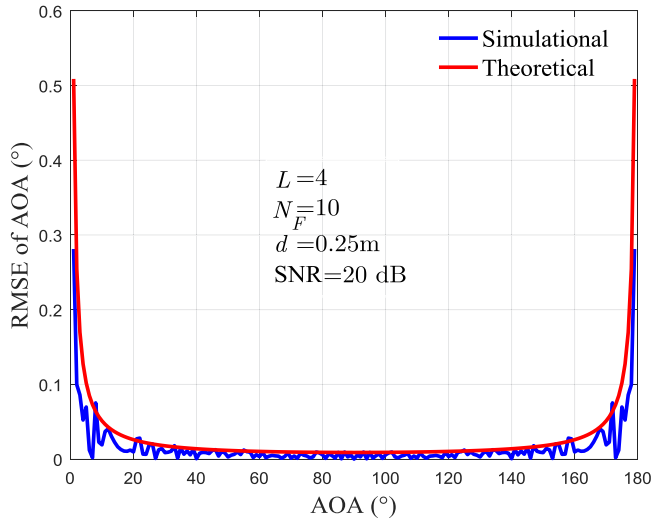


Fig. 11. RMSE of the PRIDE based AOA estimation vs AOA, $L = 4$, $N_F = 10$, $d = 0.25$ m, $\text{SNR} = 20$ dB.

interference from noise. It can be seen that the RMSE is symmetrical within $(0^\circ, 180^\circ)$ and the best performance is achieved when $\theta_u = 90^\circ$, where there is no difference between the delay time of each antenna so that a full “diversity” can be obtained. It is also observed that the RMSE fluctuates near the theoretical value, which is caused by the non-linear mapping of the TDE error by the “arccos” function in (48).

C. Computational Complexity

The evaluation of computational complexity for the PRIDE method is carried out in this sub-section. Since the PRIDE method consists of two steps for the integer and fractional delay estimation, its computational complexity can be obtained as the sum complexity of these two steps.

Taking the number of complex multiplications as the measurement, the computational complexity of the integer delay estimation is given as

$$C_{\text{PRIDE-I}} = \mathcal{O}(N(N-1)). \quad (54)$$

And the computational complexity of the fractional delay estimation can be approximated as

$$C_{\text{PRIDE-F}} = \mathcal{O}\left((1 + N_F P_u)N + \left(\frac{N_F}{2} + 1\right)N \log N\right). \quad (55)$$

Given (54) and (55), the computational complexity of the proposed PRIDE is then given as

$$C_{\text{PRIDE}} = \mathcal{O}\left(N\left(N + N_F P_u + \left(\frac{N_F}{2} + 1\right) \log N\right)\right). \quad (56)$$

Considering the traditional methods, the computational complexity of the FPS-CC estimator can be approximated as

$$C_{\text{FPS-CC}} = \mathcal{O}(N(N-1)), \quad (57)$$

and the computational complexity of the GS-ML estimator is

$$C_{\text{ML}} = \mathcal{O}\left((P_u^2 N + P_u^3 + 2N P_u + P_u^2 + P_u) N_{\text{ML}}^{P_u}\right), \quad (58)$$

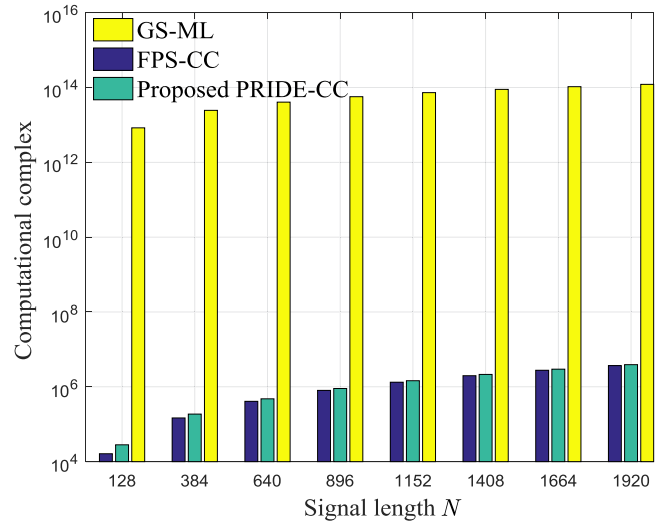


Fig. 12. Computational complexity of the proposed PRIDE-CC method.

where N_{ML} is the number of searching points, which is inversely proportional to the estimation resolution. According to (56), (57) and (58), the comparison of computational complexity among the proposed PRIDE method and the traditional methods are shown in Fig. 12, where $P_u = 5$, $N_F = 10$, and $N_{\text{ML}} = 128$. It can be seen that, the computational complexity of the proposed PRIDE is slightly higher than FPS-CC, while it is much lower than GS-ML.

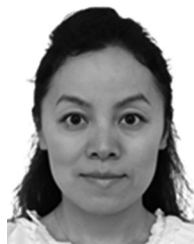
VII. CONCLUSIONS

In this paper, we have proposed a PRIDE method to obtain the delay estimation in the multi-device multi path environment. For the first time, the unique delay structure of each device has been considered and utilized. In this way, the MPI which generally hinders the TDE has been used to improve the estimation accuracy. The PRIDE method has been proposed in two steps to obtain the integer and fractional delay estimation in sequence. Theoretical analysis and simulations have been carried out to show that the accuracy of delay estimation in the multi-device multi-path environment has been greatly improved by the PRIDE method. In addition, when PRIDE is applied for AOA estimation, the spatial diversity has also been used and the RMSE decreases as the number of antennas increases.

REFERENCES

- [1] J. Choi, J. Kim, and N. S. Kim, “Robust time-delay estimation for acoustic indoor localization in reverberant environments,” *IEEE Signal Process. Lett.*, vol. 24, no. 2, pp. 226–230, Feb. 2017.
- [2] M. Sun, C. Le Bastard, Y. Wang, and N. Piniel, “Time-delay estimation using ESPRIT with extended improved spatial smoothing techniques for radar signals,” *IEEE Geosci. Remote Sens. Lett.*, vol. 13, no. 1, pp. 73–77, Jan. 2016.
- [3] A. Masmoudi, F. Bellili, S. Affes, and A. Ghayeb, “Maximum likelihood time delay estimation from single- and multi-carrier DSSS multipath MIMO transmissions for future 5G networks,” *IEEE Trans. Wireless Commun.*, vol. 16, no. 8, pp. 4851–4865, Aug. 2017.
- [4] J. Benesty, Y. Huang, and J. Chen, “Time delay estimation via minimum entropy,” *IEEE Signal Process. Lett.*, vol. 14, no. 3, pp. 157–160, Mar. 2007.

- [5] P. P. Moghaddam, H. Amindavar, and R. L. Kirlin, "A new time delay estimation in multipath," *IEEE Trans. Signal Process.*, vol. 51, no. 5, pp. 1129–1142, May 2003.
- [6] F. Fereidoony, S. Chamaani, S. A. Mirtaheri, and M. A. Sebt, "Continuous basis compressive time-delay estimation in overlapped echoes," *IET Signal Process.*, vol. 11, no. 5, pp. 566–571, Jul. 2017.
- [7] J. Benesty, J. Chen, and Y. Huang, "Time-delay estimation via linear interpolation and cross correlation," *IEEE Trans. Speech Audio Process.*, vol. 12, no. 5, pp. 509–519, Sep. 2004.
- [8] E. Shaswary, J. Tavakkoli, and Y. Xu, "A new algorithm for time-delay estimation in ultrasonic echo signals [Correspondence]," *IEEE Trans. Ultrason., Ferroelect., Freq. Control*, vol. 62, no. 1, pp. 236–241, Jan. 2015.
- [9] B. Park, H. Cheon, C. Kang, and D. Hong, "A novel timing estimation method for OFDM systems," *IEEE Commun. Lett.*, vol. 7, no. 5, pp. 239–241, May 2003.
- [10] C. Knapp and G. Carter, "The generalized correlation method for estimation of time delay," *IEEE Trans. Acoust., Speech, Signal Process.*, vol. ASSP-24, no. 4, pp. 320–327, Aug. 1976.
- [11] K. Gedalyahu and Y. C. Eldar, "Time-delay estimation from low-rate samples: A union of subspaces approach," *IEEE Trans. Signal Process.*, vol. 58, no. 6, pp. 3017–3031, Jun. 2010.
- [12] C. Kuglin, "The phase correlation image alignment method," in *Proc. IEEE Int. Conf. Cybern. Soc.*, 1975, pp. 163–165.
- [13] H. Choudhary, R. Bahl, and A. Kumar, "Inter-sensor time delay estimation using cepstrum of sum and difference signals in underwater multipath environment," in *Proc. IEEE Underwater Technol.*, May 2015, pp. 1–7.
- [14] F. X. Ge, D. Shen, Y. Peng, and V. O. Li, "Super-resolution time delay estimation in multipath environments," *IEEE Trans. Circuits Syst. I, Reg. Papers*, vol. 54, no. 9, pp. 1977–1986, Sep. 2007.
- [15] A. Masmoudi, F. Bellili, S. Affes, and A. Stephenne, "A maximum likelihood time delay estimator in a multipath environment using importance sampling," *IEEE Trans. Signal Process.*, vol. 61, no. 1, pp. 182–193, Jan. 2013.
- [16] H. Zhou and Y. F. Huang, "A maximum likelihood fine timing estimation for wireless OFDM systems," *IEEE Trans. Broadcast.*, vol. 55, no. 1, pp. 31–41, Mar. 2009.
- [17] M. Feder and E. Weinstein, "Parameter estimation of superimposed signals using the EM algorithm," *IEEE Trans. Acoust., Speech, Signal Process.*, vol. ASSP-36, no. 4, pp. 477–489, Apr. 1988.
- [18] F. Shang, B. Champagne, and I. N. Psaromiligkos, "A ML-based framework for joint TOA/AOA estimation of UWB pulses in dense multipath environments," *IEEE Trans. Wireless Commun.*, vol. 13, no. 10, pp. 5305–5318, Oct. 2014.
- [19] I. Guvenc, S. Gezici, and Z. Sahinoglu, "Ultra-wideband range estimation: Theoretical limits and practical algorithms," in *Proc. IEEE Int. Conf. Ultra-Wideband*, Oct. 2008, vol. 3, pp. 93–96.
- [20] H. Ni, G. Ren, and Y. Chang, "A TDOA location scheme in OFDM based WMANs," *IEEE Trans. Consum. Electron.*, vol. 54, no. 3, pp. 1017–1021, Aug. 2008.
- [21] Y. Huang, A. Hu, Y. Huang, S. Xie, D. Zhu, and M. Xue, "An integer time delay estimation algorithm based on Zadoff-Chu sequence in OFDM systems," *IEEE Trans. Veh. Technol.*, vol. 63, no. 6, pp. 2941–2947, Jul. 2014.
- [22] J. Zhu, R. Schober, and V. K. Bhargava, "Secure transmission in multicell massive MIMO systems," *IEEE Trans. Wireless Commun.*, vol. 13, no. 9, pp. 4766–4781, Sep. 2014.
- [23] L. Taponnecco, A. A. D'Amico, and U. Mengali, "Joint TOA and AOA estimation for UWB localization applications," *IEEE Trans. Wireless Commun.*, vol. 10, no. 7, pp. 2207–2217, Jul. 2011.
- [24] A. A. D'Amico, U. Mengali, and L. Taponnecco, "TOA estimation with the IEEE 802.15.4a standard," *IEEE Trans. Wireless Commun.*, vol. 9, no. 7, pp. 2238–2247, Jul. 2010.
- [25] S. Mota, F. Perez-Fontan, and A. Rocha, "Estimation of the number of clusters in multipath radio channel data sets," *IEEE Trans. Antennas Propag.*, vol. 61, no. 5, pp. 2879–2883, May 2013.
- [26] Y. Gu and N. A. Goodman, "Information-theoretic compressive sensing kernel optimization and Bayesian crammer-Rao bound for time delay estimation," *IEEE Trans. Signal Process.*, vol. 65, no. 17, pp. 4525–4537, Sep. 2017.
- [27] R. Schmidt, "Multiple emitter location and signal parameter estimation," *IEEE Trans. Antennas Propag.*, vol. AP-34, no. 3, pp. 276–280, Mar. 1986.
- [28] R. Roy and T. Kailath, "ESPRIT-estimation of signal parameters via rotational invariance techniques," *IEEE Trans. Acoust., Speech, Signal Process.*, vol. 37, no. 7, pp. 984–995, Jul. 1989.



Wei Peng (M'07–SM'12) received the Ph.D. degree in wireless communications from the University of Hong Kong, Hong Kong, in 2007. She was with Tohoku University, Sendai, Japan, as a Post-Doctoral Research Fellow from 2008 to 2009 and an Assistant Professor from 2009 to 2013. Since 2013, she has been with the School of Electronic Information and Communications, Huazhong University of Science and Technology, Wuhan, China, as an Associate Professor. She held a visiting position in Columbia University, New York, NY, USA. Her research interests include signal processing for large-scale wireless communication systems, online learning based network optimization, and space-ground integrated network.



Xuehui Zhao is currently working toward the master's degree with the School of Electronic Information and Communications, Huazhong University of Science and Technology, Wuhan, China.



Tao Jiang (M'06–SM'10) received the Ph.D. degree in information and communication engineering from the Huazhong University of Science and Technology, Wuhan, China, in 2004. He is currently a Distinguished Professor with the School of Electronic Information and Communications, Huazhong University of Science and Technology. From 2004 to 2007, he was with some universities including Brunel University and University of Michigan-Dearborn. He has authored or coauthored about 300 technical papers in major journals and conferences and 9 books/chapters in areas of communications and networks. He is an Associate Editor for some technical journals in communications including the IEEE TRANSACTIONS ON SIGNAL PROCESSING, the IEEE COMMUNICATIONS SURVEYS AND TUTORIALS, the IEEE TRANSACTIONS ON VEHICULAR TECHNOLOGY, the IEEE INTERNET OF THINGS JOURNAL, etc.



Fumiuyuki Adachi (M'79–SM'90–F'02–LF'16) received the B.S. and Dr. Eng. degrees in electrical engineering from Tohoku University, Sendai, Japan, in 1973 and 1984, respectively. In April 1973, he joined the NTT company and conducted research on digital cellular mobile communications. From 1992 to 1999, he was with NTT DOCOMO, where he led a research group on wideband/broadband wireless access for 3G and beyond. Since 2000, he has been a Full Professor with the Department of Communications Engineering, Tohoku University until March 2016. Currently, he is a Specially Appointed Professor with the Research Organization of Electrical Communication, Tohoku University. His research interests are in the area of wireless signal processing and networking.